X-ray Instruments

Space Instrumentation (ELEC-E4220)

Karri Koljonen

The Finnish Centre for Astronomy with ESO; Aalto University Metsähovi Radio Observatory

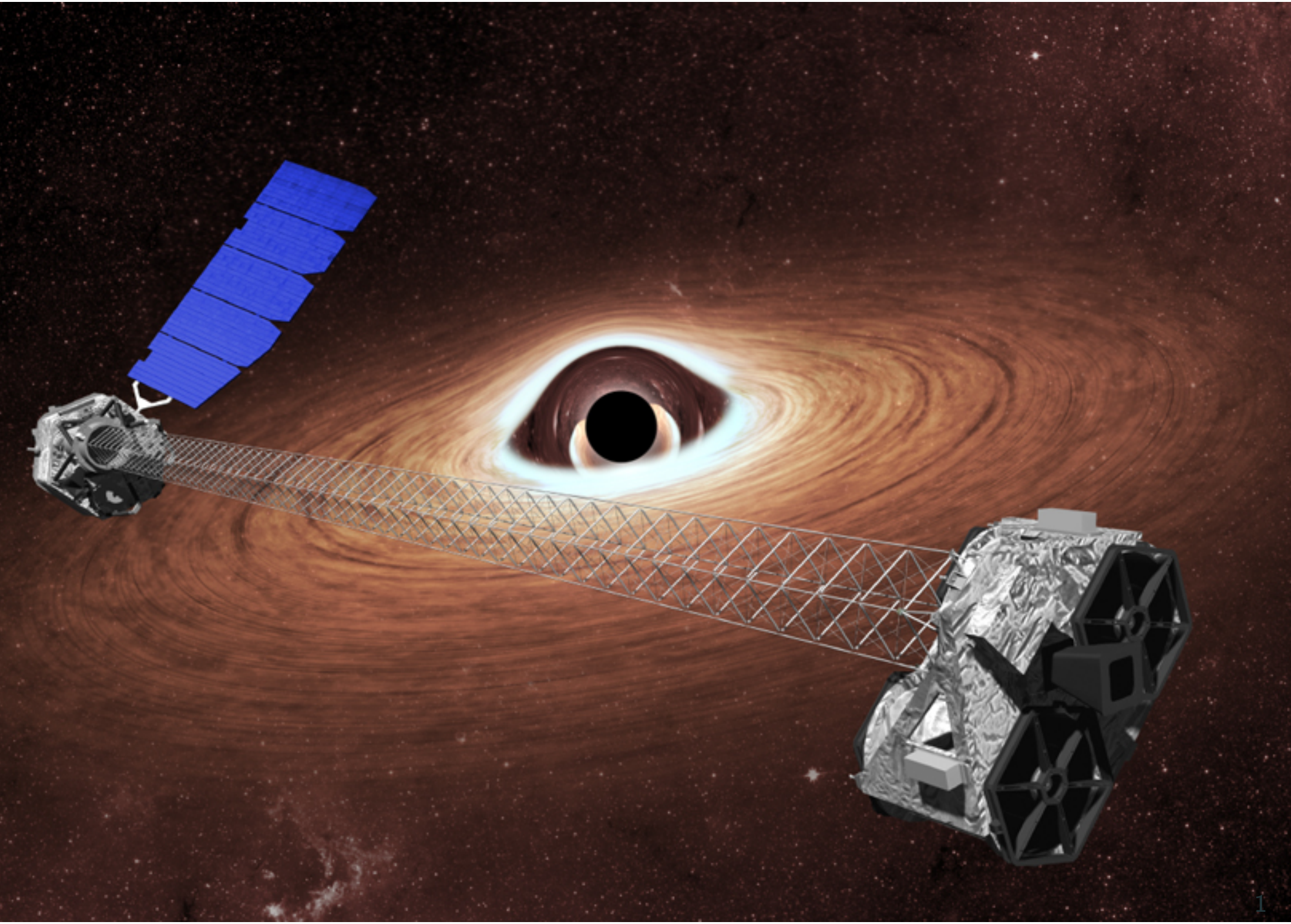

Table of contents

Introduction

X-rays

Light can be characterized by:

Wavelength (λ)
measured in m, mm, cm, nm, Å.

Frequency (ν)
measured in Hz, MHz, GHz.

Energy (E)
measured in J, erg, Rydbergs, eV, keV, MeV, GeV.

Temperature (T)
measured in K.

That are related as:

$$\lambda\nu = c \qquad E = h\nu \qquad T = E/k \tag{1}$$

c = speed of light, h = Planck constant, k = Boltzmann constant.

X-rays (my definition): 100–0.1 Å (10-0.01 nm), 3×10^{16}–3×10^{19} Hz, 0.1–100 keV, 10^6–10^9 K.

X-rays

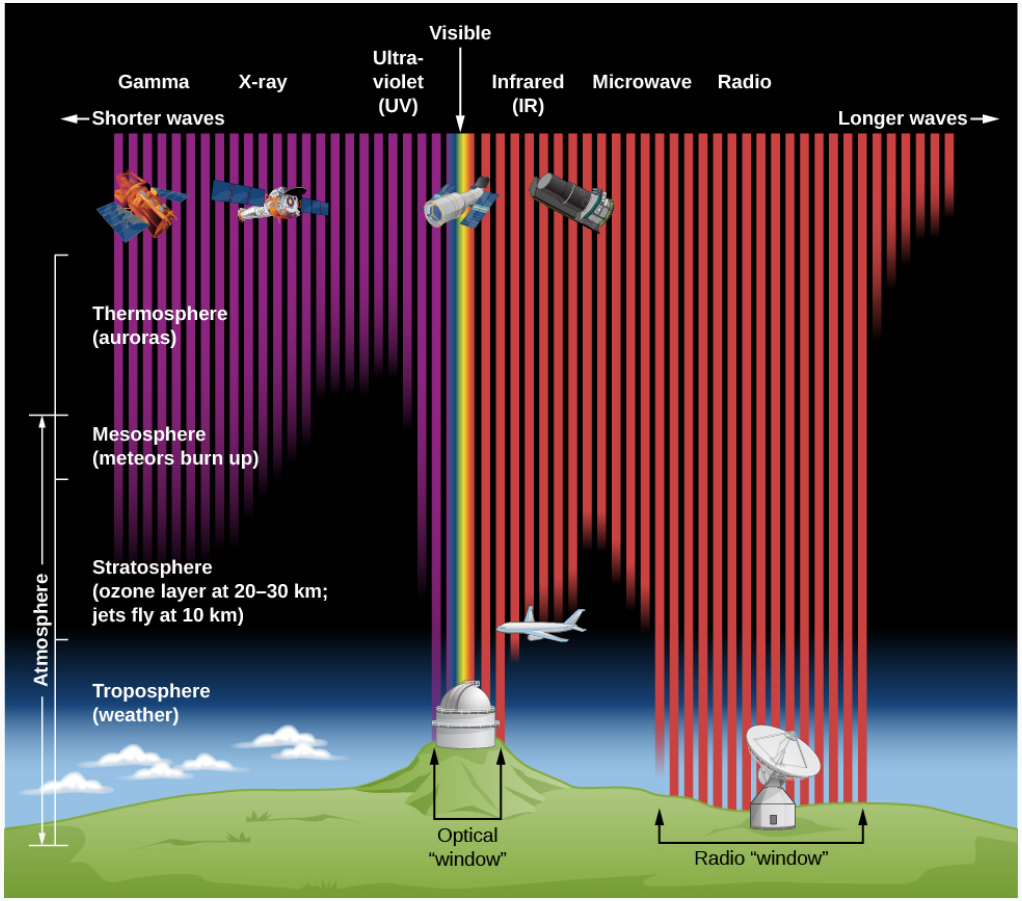

Picture credit: STScI/JHU/NASA

X-rays: Nobel mania

1901: Very first Nobel prize in physics to Wilhelm Röntgen.

1914: Max von Laue for X-ray diffraction by crystals.

1915: Father and son Bragg for X-ray crystallography – imaging molecular structures (used by Watson & Crick in imaging DNA + 25 other N. prize winners).

1992: G. Charpak for the invention of multiwire proportional chamber.

2002: Riccardo Giacconi for pioneering contributions to astrophysics, discovery of cosmic X-ray sources.

X-ray astronomy

Why X-rays?

- They reveal the existence of astrophysical processes where matter has been heated to temperatures of millions of degrees or in which particles have been accelerated to relativistic energies.
- Numerous compared to γ-rays.
- Penetrate cosmological distances.
- They can be focused by special telescopes.

  The Universe we know today is pervaded by the echoes of enormous explosions and rent by abrupt changes of luminosity on large energy scales. From the initial explosion to formation of galaxies and clusters, from the birth to the death of stars, high energy phenomena are the norm and not the exception in the evolution of the Universe. – Riccardo Giacconi

History: Milestones

1946: First discovery of X-rays from the Sun by Friedmann et al. (Using left-over V2 rockets).

1962: Giacconi & Rossi tried to see the fluorescence of solar X-rays from the Moon, but discovered a very bright source: Sco X-1.

1970: First X-ray satellite UHURU discovered many bright sources (total of 339), e.g. Cyg X-1 (evidence for a black hole). X-ray emission from galaxy clusters.

1974: Ariel 5, X-ray emission in Seyfert galaxies, closest X-ray binary outburst: A0620–00.

1983: EXOSAT, first European satellite. Variability in X-ray emission from Seyfert galaxies = supermassive black holes. Galactic ridge emission.

1990: ROSAT, Germany/UK/USA satellite, >100k sources.

1999: XMM-Newton (>500k sources), Chandra (>300k sources).

History: Major X-ray satellite missions over time

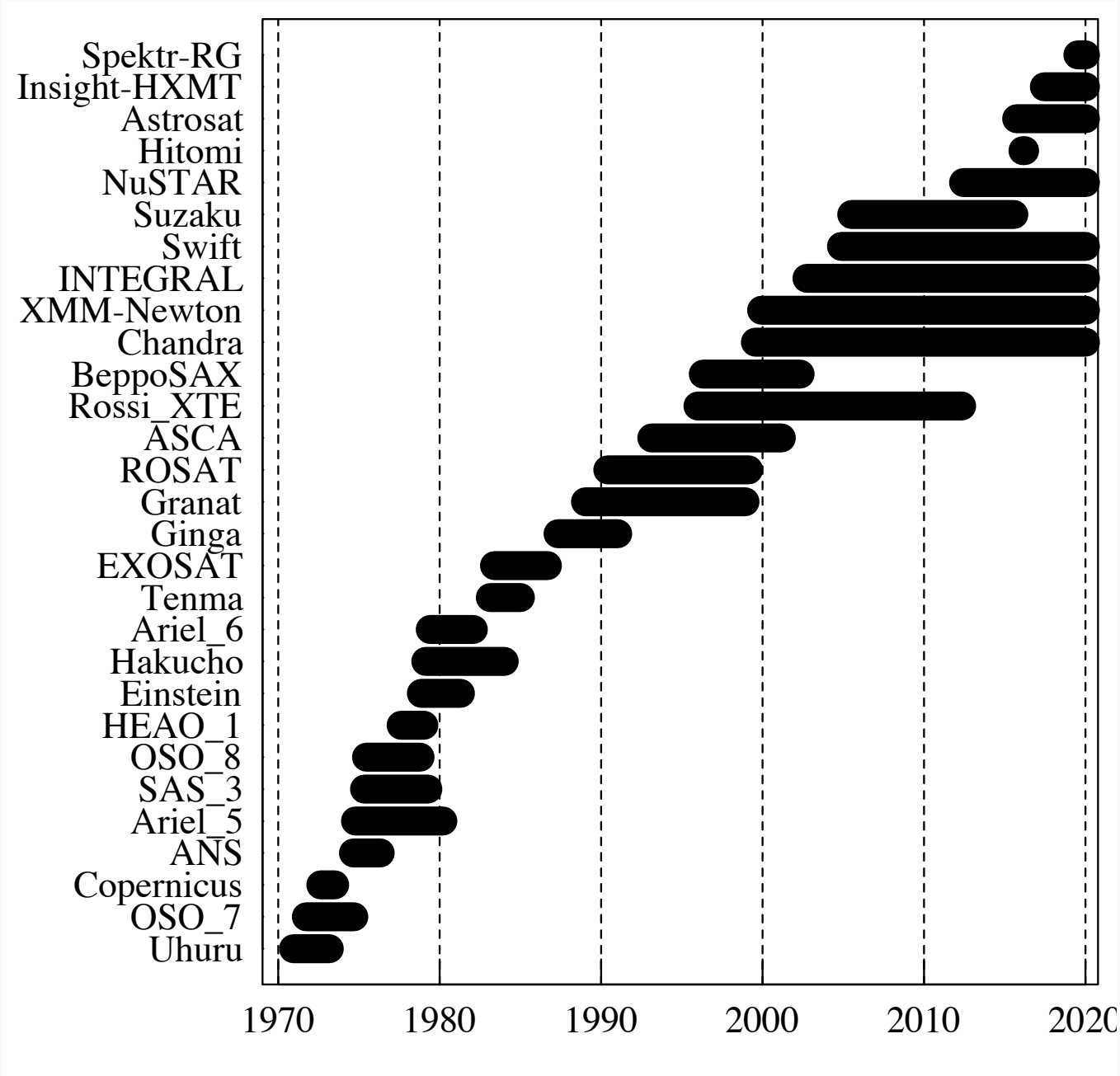

Current X-ray satellite fleet

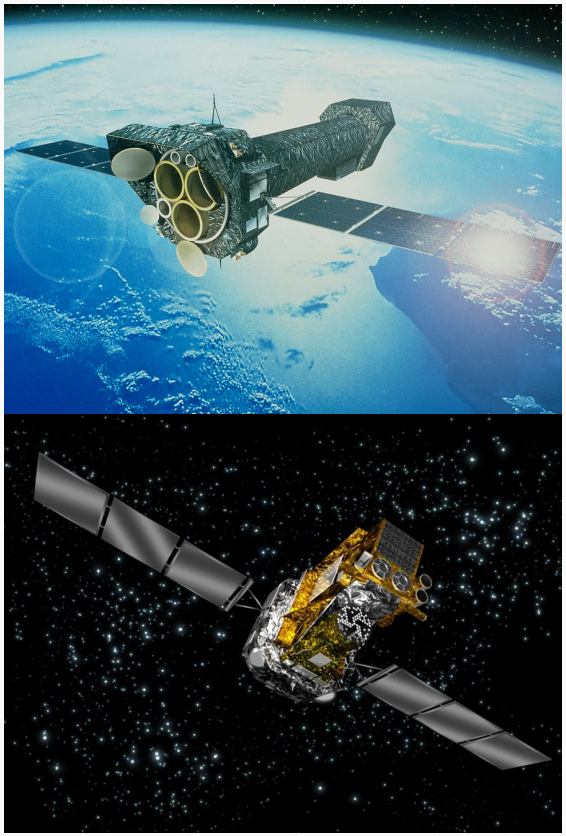

ESA fleet:
XMM-Newton (*top*),
INTEGRAL (*bottom*)

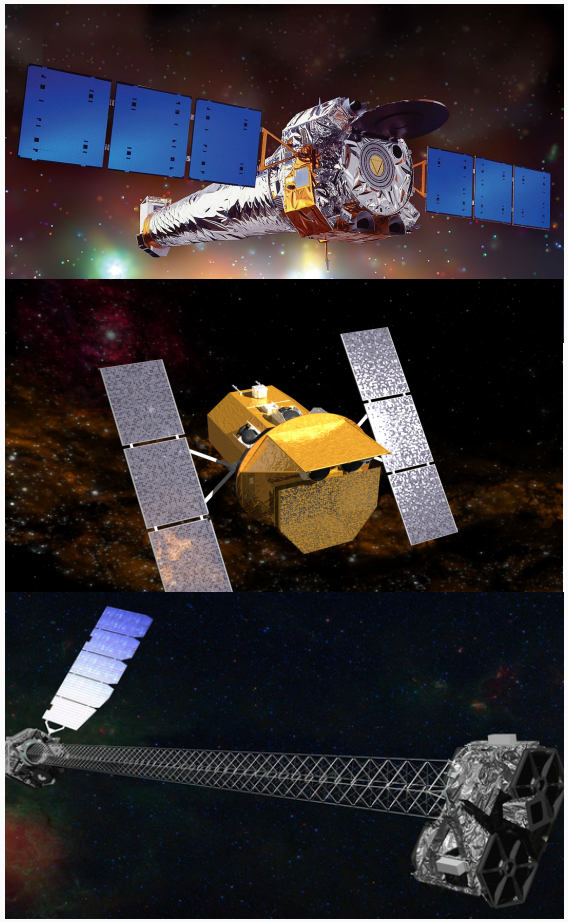

NASA fleet: Chandra (*top*), Swift (*middle*), NuSTAR (*bottom*)

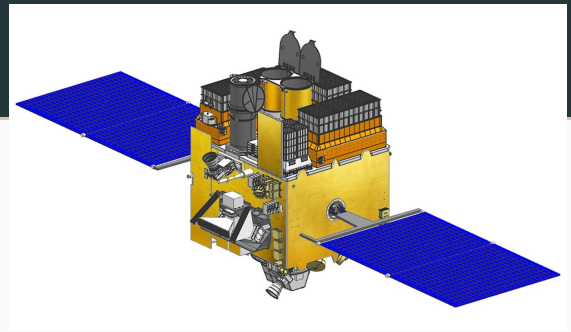

Astrosat (ISRO)

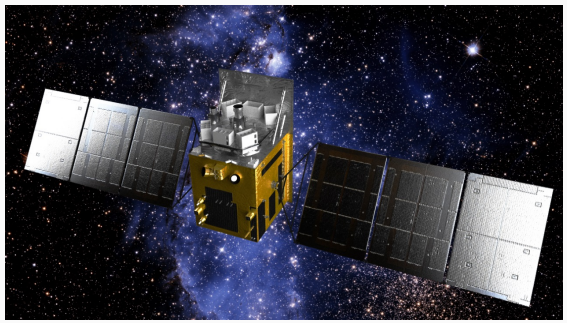

Insight-HXMT (CAS)

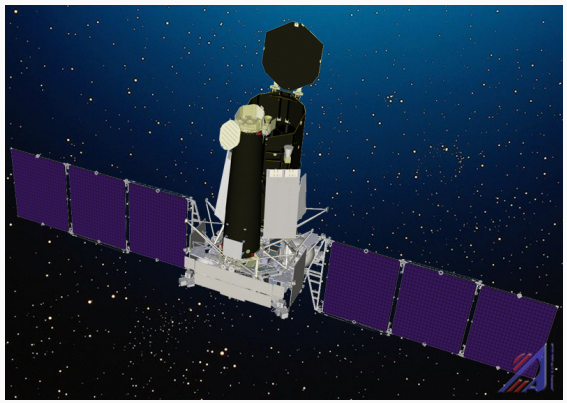

Spektr-RG (MPE/IKI RAS)

+ 2 instruments (NICER, MAXI) on ISS.

The number of detected X-ray sources

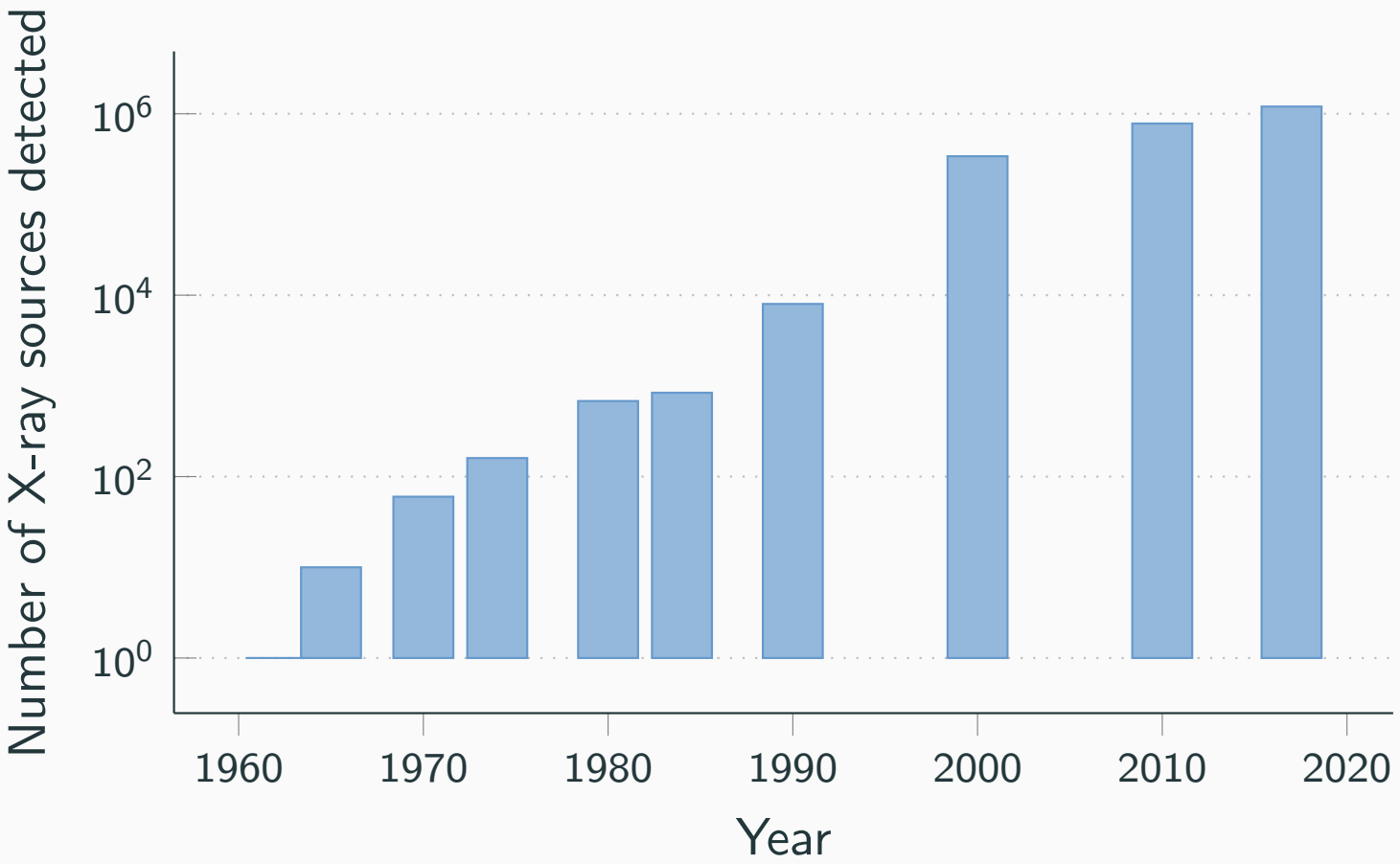

XMM all-sky map

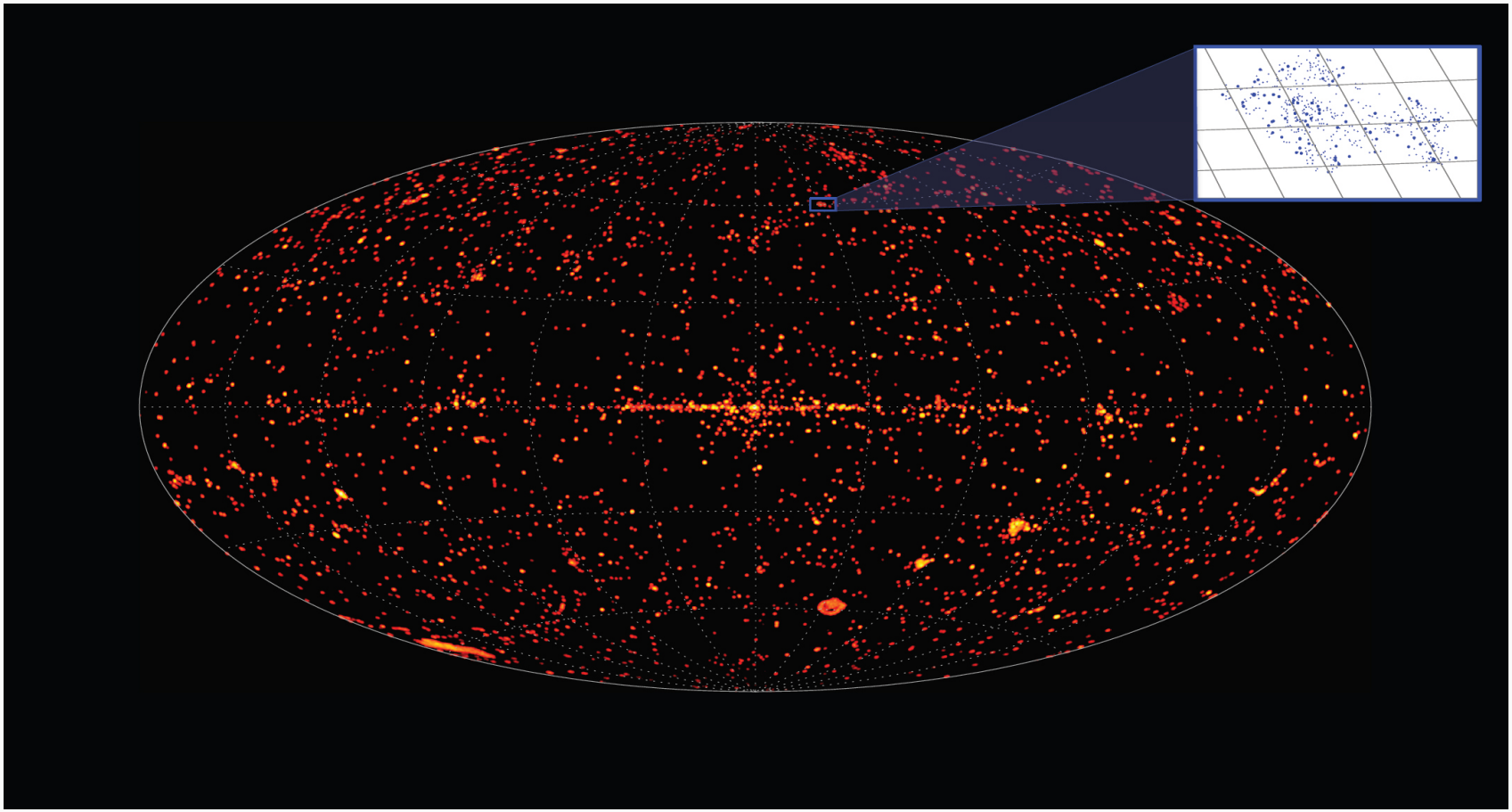

ESA/XMM-Newton/EPIC/M. Watson (University of Leicester)

X-ray sources

Black hole & neutron star X-ray binaries, ultra-luminous X-ray binaries, pulsars, gamma-ray bursts (gravitational wave counterparts!), supernova remnants, magnetars, white dwarfs, brown dwarfs, young stars, massive stars, galaxy clusters, quasars, starburst galaxies, interstellar medium, diffuse X-ray background ...



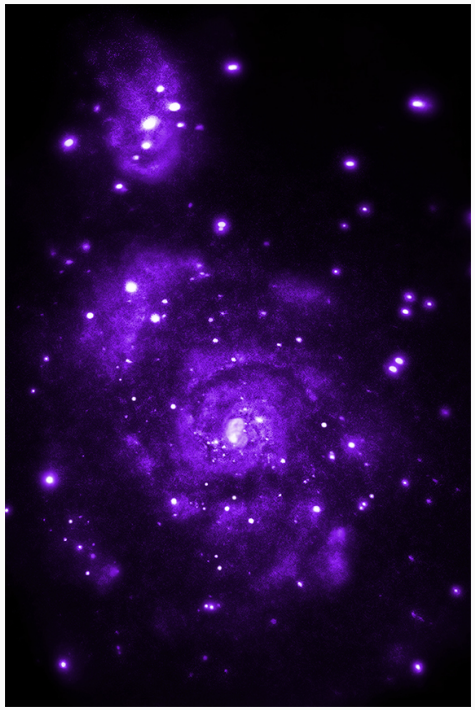
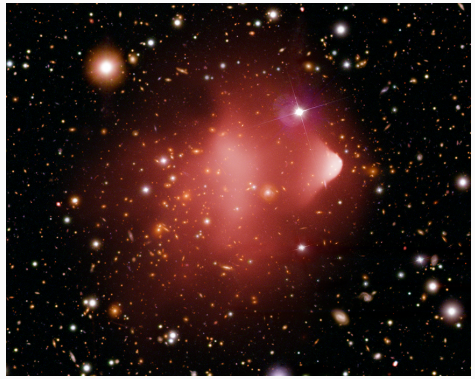

Picture credits: NASA/CXC

Detecting X-rays

Distance effects

Object	Distance (pc)	Flux (erg/s/cm^2)	Luminosity (erg/s)
One-megaton nuclear bomb			4×10^{22}
Solar system:			
Very large solar flare	5×10^{-6}	7	2×10^{28}
Galactic:			
Active young star (AB Dor)	10	4×10^{-9}	1×10^{32}
Cataclysmic binary (SS Cyg)	75	5×10^{-11}	3×10^{31}
Supernova remnant (Crab nebula)	2000	6×10^{-8}	3×10^{37}
X-ray binary (Sco X-1)	2800	2×10^{-7}	2×10^{38}
Magnetar flare (SGR 1806-20)	15000	5	1×10^{47}
Extragalactic:			
Active Galactic Nucleus (M87)	22×10^{6}	5×10^{-10}	3×10^{46}
Gamma-ray burst (GRB 100621A)	1×10^{9}	3×10^{-6}	3×10^{51}

Counting photons

Object	Flux (erg/s/cm^2)	Photon flux (X-ray photons/s/cm^2)
Solar system:		
Very large solar flare	7	2.5×10^9
Galactic:		
Active young star (AB Dor)	4×10^{-9}	1.4
Cataclysmic binary (SS Cyg)	5×10^{-11}	0.02
Supernova remnant (Crab nebula)	6×10^{-8}	21
X-ray binary (Sco X-1)	2×10^{-7}	71
Magnetar flare (SGR 1806-20)	5	1.8×10^9
Extragalactic:		
Active Galactic Nucleus (M87)	5×10^{-10}	0.18
Gamma-ray burst (GRB 100621A)	3×10^{-6}	1100

Detectors

Originally Geiger-counters in rockets, **proportional counters** in rockets, balloons and satellites (still used today). **CCDs** and **micro-calorimeters** in more modern detectors. Other designs (not dealt with here): e.g. micro-channel plates, scintillators (mainly γ-ray detectors).

Five important factors for the detector design:

(1) **Counting (photometry)**: We need to detect single photons. This means heavy amplification of the signal.

(2) **Counting fast (timing)**: Recording the arrival time of single photons. Requires fast signal processing.

(3) **Weighing (spectrometry)**: We want to measure the energy of the photon.

(4) **Locating (imaging)**: We want to know where the photon came from.

(5) **Polarity (polarimetry)**: Are the photons polarized and in what way? Will give us hints about the emission mechanisms.

Proportional counters

Ionization chambers, i.e. a bucket of gas, containing two electrodes that have potential difference of several hundreds of volts.

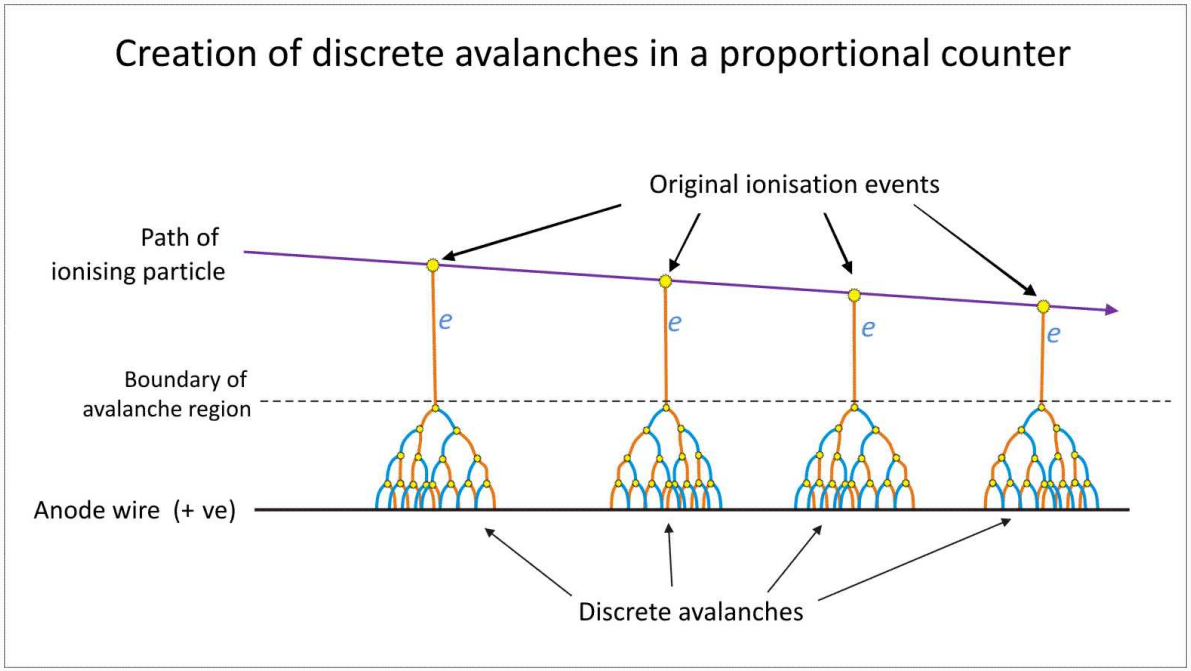

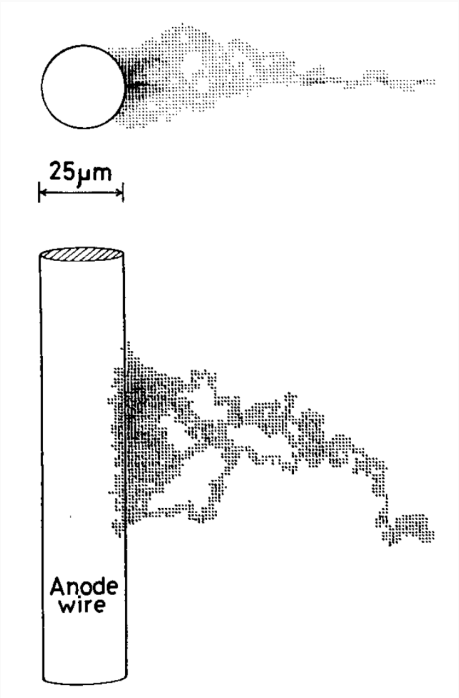

Number of ionization events depends on initial energy of the photon. One ionization event in the tube results in 10^4–10^6 ion pairs. Produces intense pulse of current that can be measured as a *count event*. Signal duration $\sim$ 100 μs.

Proportional counters II

Pulse height: ΔQ = -Ne = $C\Delta U$

Measured voltage (including amplification from avalanches):

$$\Delta U = -\frac{Ne}{C} \times A = -\frac{2 \times 10^5 e^- \times e}{20pF} \times 10^4..10^6 \approx 16..1600V \qquad (2)$$

Since A is known ($\sim$ const.) and voltage pulse $\propto$ N, therefore

Voltage pulse $\propto$ energy of the X-ray photon.

Proportional counters III

Detector gas usually argon or xenon. **Why?** Inert gases, required voltage is smallest and low losses due to excitation of the gas atoms.

Number of ions produced: $N = E_{X-ray\ photon}/\omega$. ω = average ionization energy.

Gas	H	He	Ne	Ar	Kr	**Xe**	Air	CO_2	CH_4
ω [eV]	36.6	44.4	36.8	26.3	24.1	**21.9**	35.2	34.2	29.1

$\rightarrow$ N $\sim$ 1000 ion pairs for 20 keV photon.

Note (1): The probability of photo-absorption depends on the size of the nucleus: $\sigma \propto Z^{4..5}$ (Argon = 18, Krypton = 36, Xenon=54).

Note (2): The probability of photo-absorption depends on the energy of the photon: $\sigma \propto E^{-3}$ (limited to <100 keV).

Proportional counters IV

Upscaling: using multiwire proportional counters (Nobel prize - Charpak 1992). Many detectors in the same gas volume. Positioning parallel anode wires about 2 mm apart between cathode planes. Each wire will act as an independent detector.

- Increase in detector area leads to increase in the number of detected photons = more sensitivity.
- Increase in the position resolution ($\sim$ wire spacing in the perpendicular direction). Resolution in the parallel direction can be measured using charge division at the both ends of the anode lines.

Stacking: Increase in position resolution (track the particle path). Increase in energy resolution (higher energy photons penetrate deeper).

Proportional counters IV

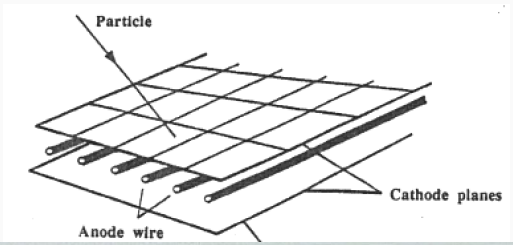

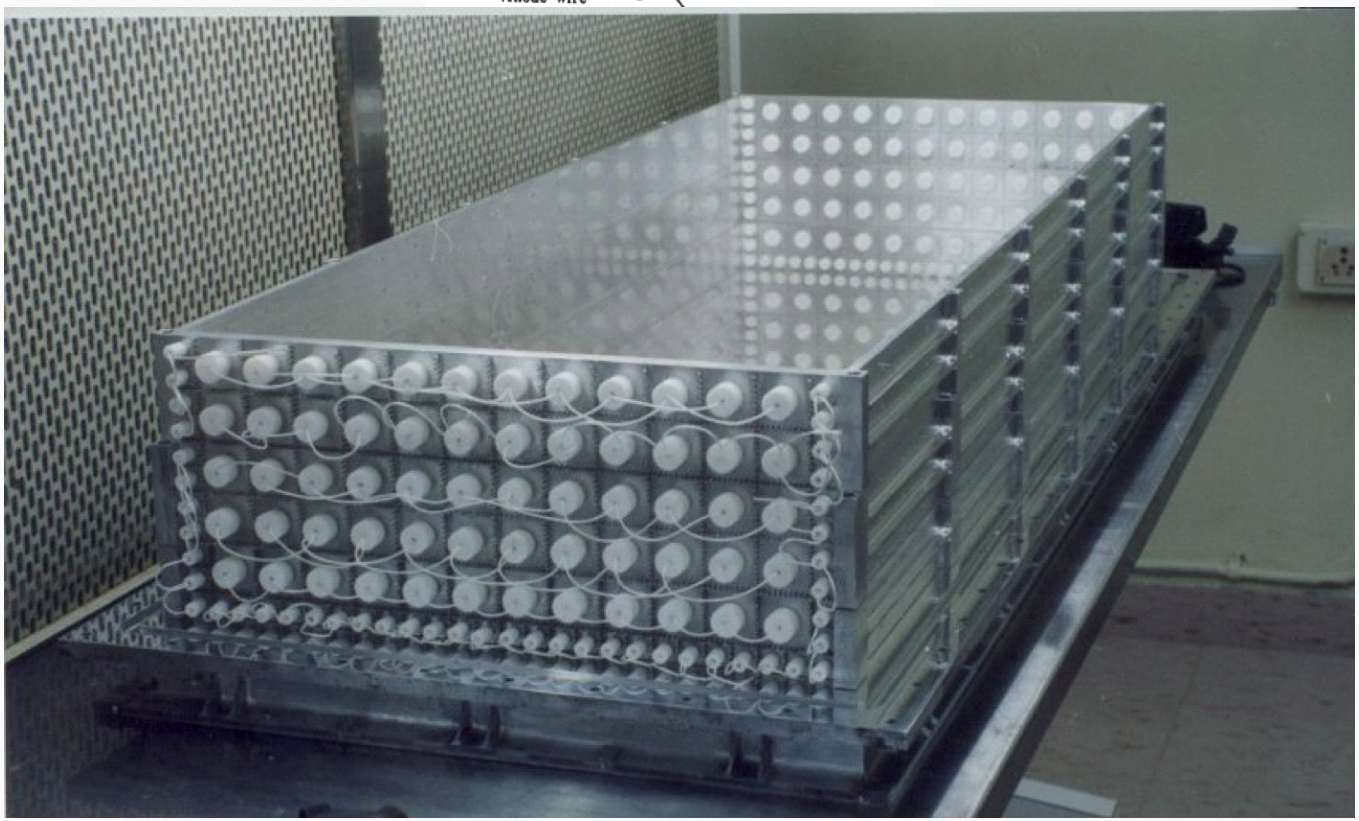

Astrosat/LAXPC

Proportional counters: Conclusion

Pros: Large collecting area, high time resolution, high counting rates, low power (no detector cooling)

Cons: Poor spatial resolution, poor spectral resolution. Mechanically very sensitive, physical and chemical breakdown of gases, ageing.

Counting $\rightarrow$ Poisson statistics ($\Delta N = \sqrt{N}$). The width of the distribution of measured energies (i.e. spectral resolution): $\Delta E/E \sim 2.35 \Delta N/N = 2.35/\sqrt{N} \sim 2.35/\sqrt{E}$. In reality $\Delta E/E \sim 5 - 20\%$. Producing charge is not completely independent as the number of ways an atom may be ionized is limited by the discrete electron shells = Fano factor. Also, the energy to produce a charge is material dependent.

Spectral range: 1-100 keV

Example: RXTE, AstroSat

Proportional counters: Future

?

New, ambitious mission designs do not really consider proportional counters. Solid-state detectors are the norm nowadays.

Semiconductor detectors I

In a solid, electrons have allowed and forbidden bands of energy. In semi-conductor the lower energy level is full and forbidden gap is reduced so that an electron may be exited across it by absorbing a photon.

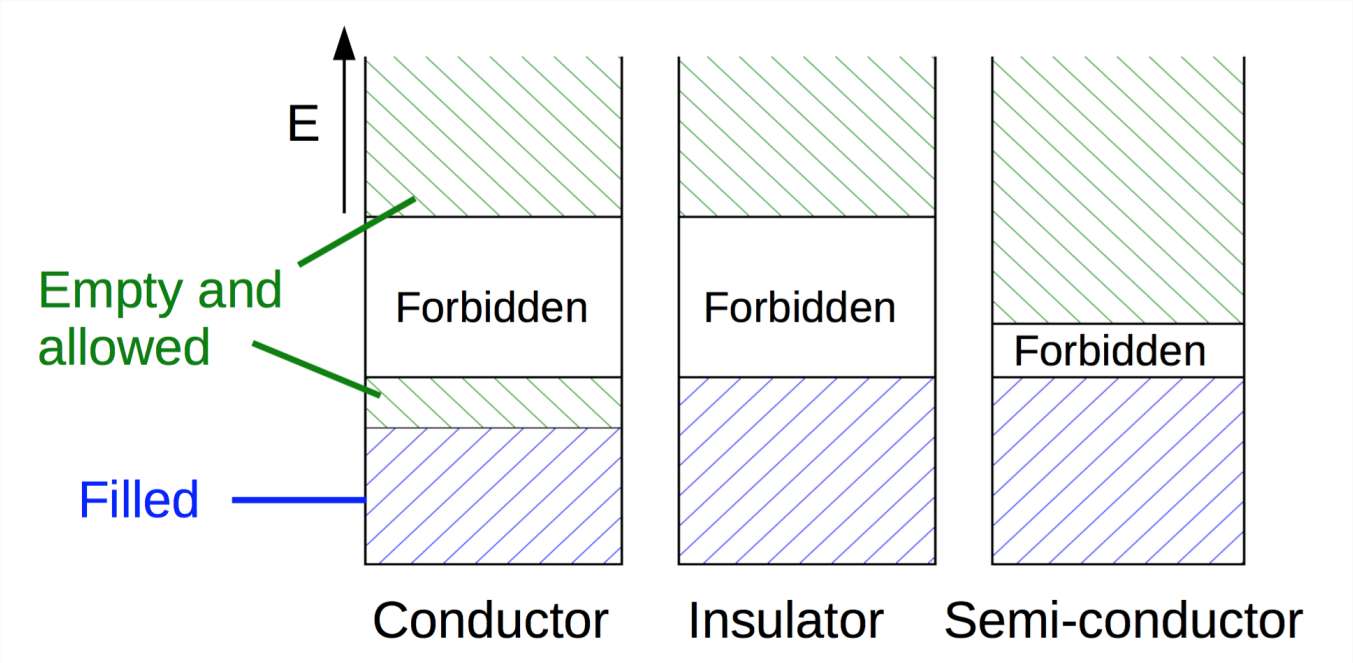

Semiconductor detectors II

Using CCDs as a solid state ionization chambers: The photon that strikes the semi-conductor free electrons producing a charge which is stored by applying an electric field. For the electron to jump over the forbidden gap in semiconductor it needs $\sim$1 eV of energy. Number of electrons produced:

$$N \sim \frac{h\nu}{E_{gap}} \tag{3}$$

Thus, for visible light $h\nu_{opt} \sim E_{gap}$ and ~ 1 electron is produced. For X-rays, $h\nu_X \sim 1000\, E_{gap}$ resulting to ~ 1000 electrons/photon.

Note: Since forbidden gap is small, semiconductor needs to be cooled to reduce thermal noise.

Semiconductor detectors III

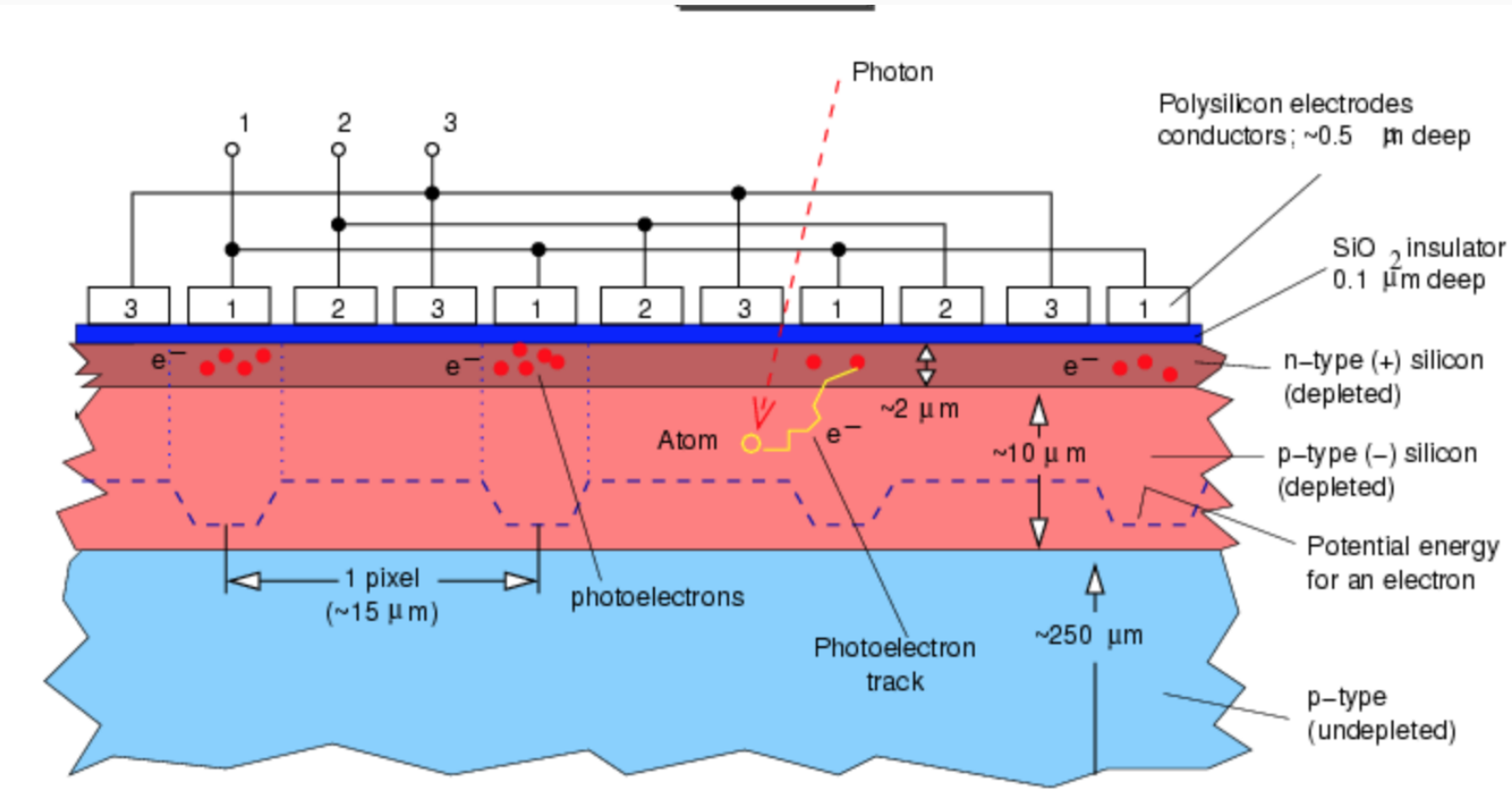

After Bradt

Semiconductor detectors IV

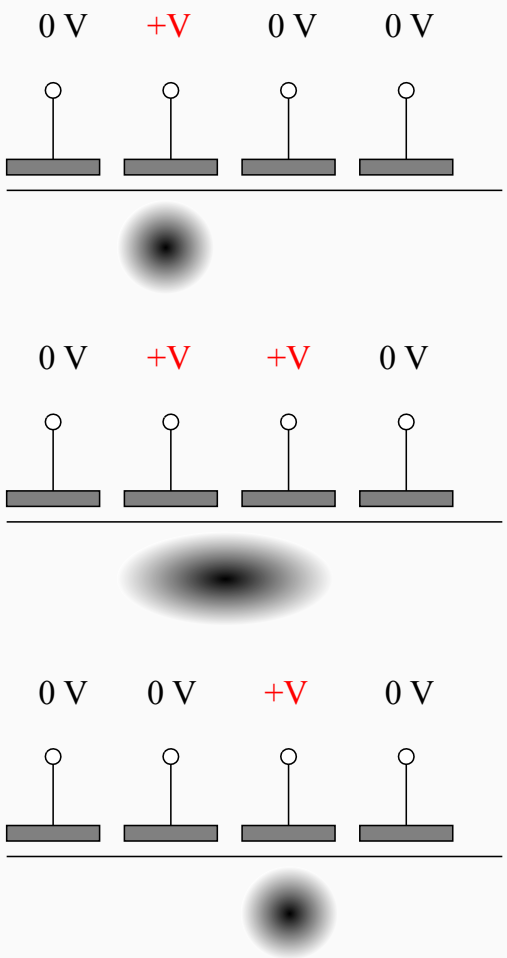

Charge is transferred by applying a modulating voltage to the electrodes.

Semiconductor detectors V

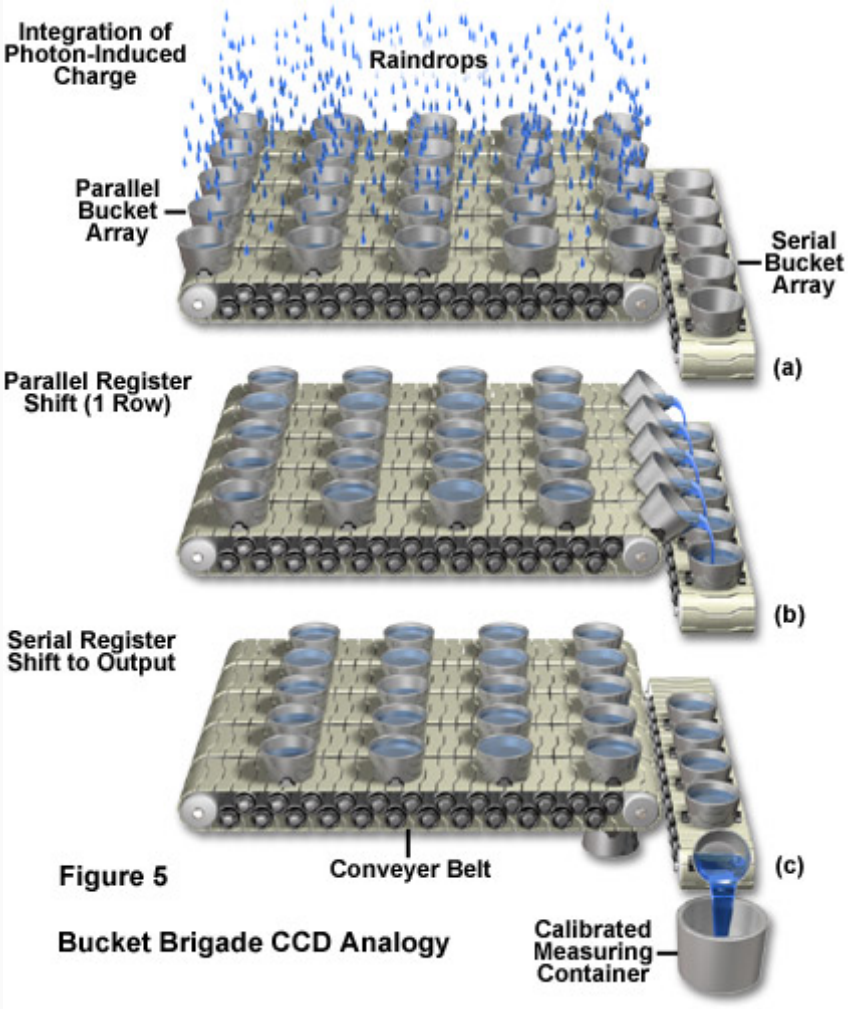

Signal is collected at one corner, amplified and digitized, or having one amplifier and analog-to-digital converter per row (expensive).

Semiconductor detectors VI

Detector with 100 x 100 pixels, background level 1 photon/pixels/s, source flux 0.2 photon/pixel/s.

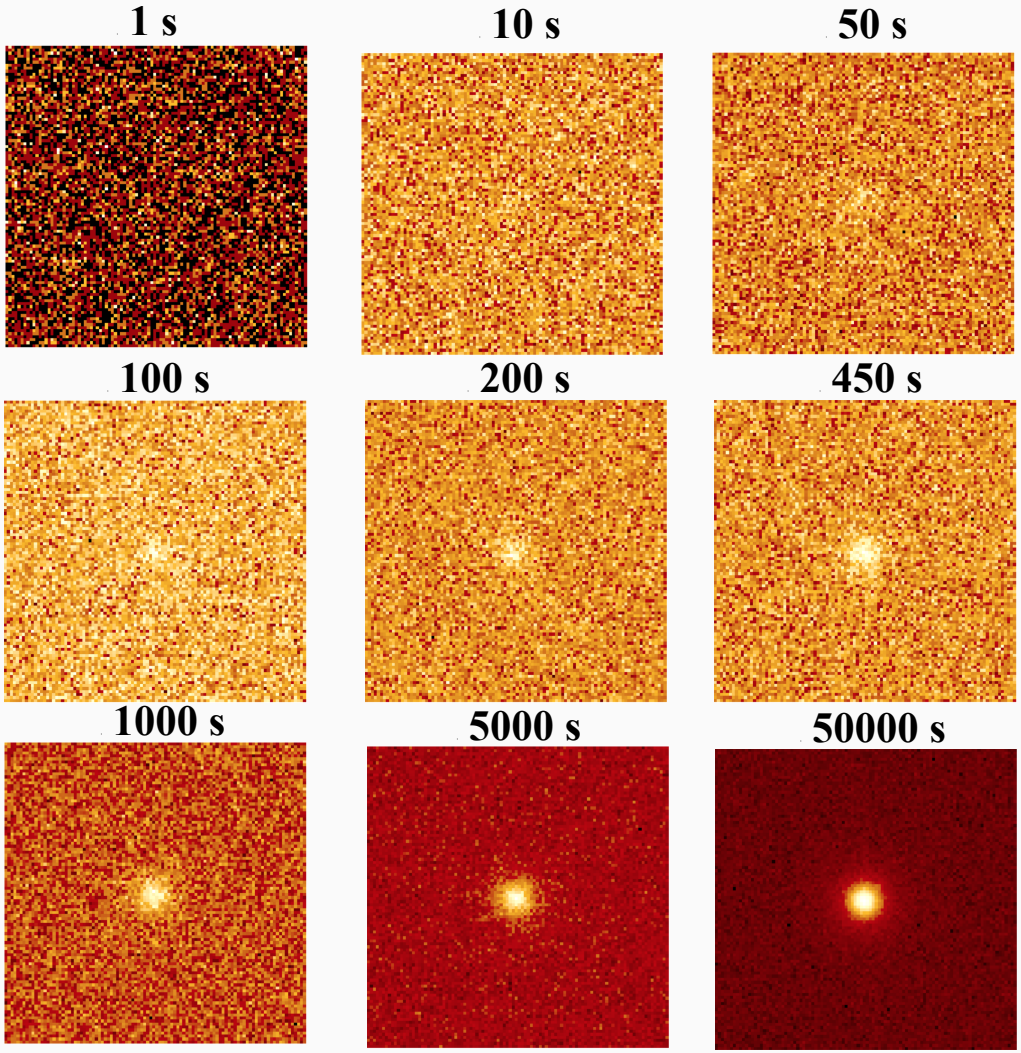

Semiconductor detectors VII

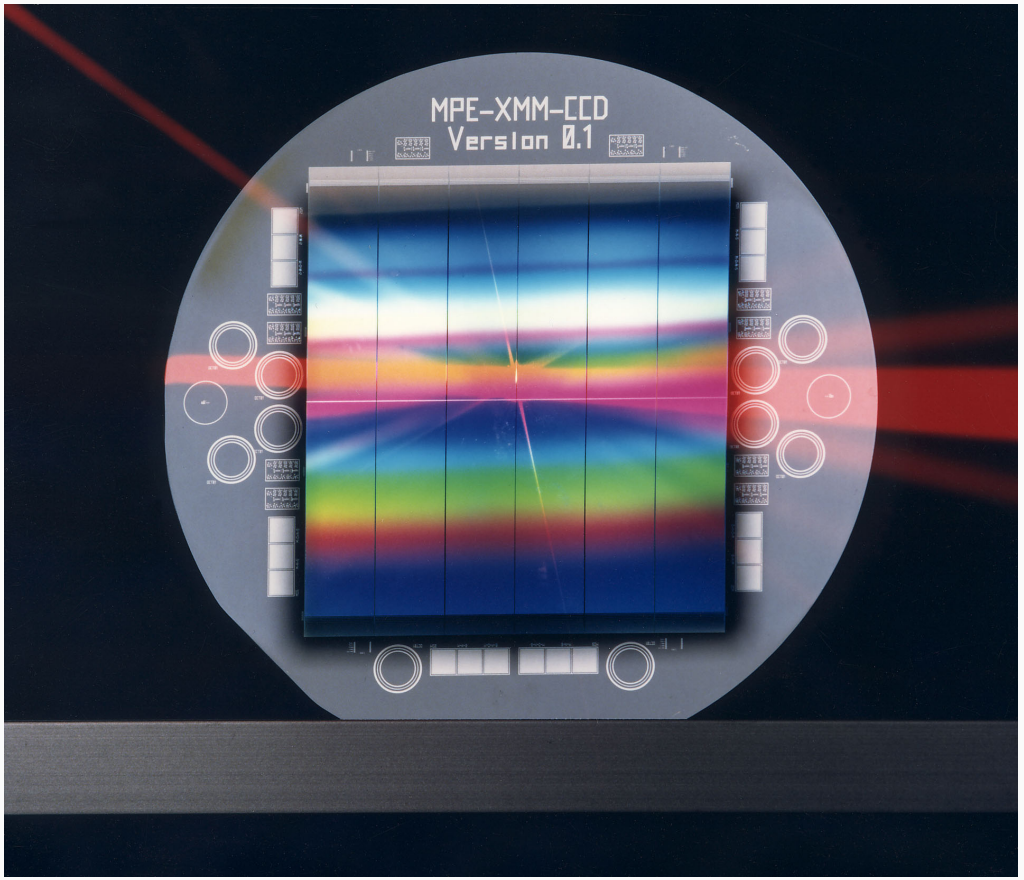

XMM-Newton EPIC-pn CCD. 12 3×1 cm backside illuminated CCDs on a single wafer. At the time of production one of the most complex Silicon structures ever made.

Semiconductor detectors: Conclusion

Pros: Imaging, spectral line studies possible, very sensitive ($\sim$100%).

Cons: Limits to energy resolution (but better compared to proportional counters), slow readout, "pile-up", relatively high background (compared to gas), susceptible to radiation damage.

Poisson statistics: Basically, the same applies as for proportional counters ($\Delta E/E \propto 2.35\sqrt{E}$). $\Delta E/E \sim$ 0.5%–5%, because of better Fano factors and different detector material.

Spectral range: historically 0.1–10 keV, but modern semiconductors can reach up to 80 keV (NuSTAR).

Example: Chandra, XMM-Newton, Suzaku, NuSTAR.

Is and will be the "workhorse" detector for future X-ray satellites.

Semiconductor detectors: Future

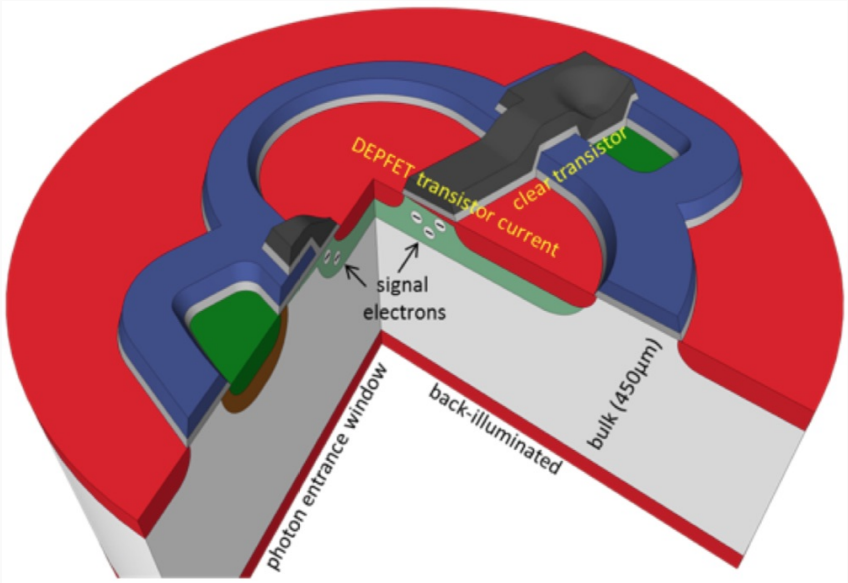

Launch in early 2030's, ESA's large-class mission *Athena* (Advanced Telescope for High ENergy Astrophysics) X-ray observatory will have two focal plane instruments, one being the Wide Field Imager (WFI) containing a solid-state detector consisting of active pixel sensors (DEPFET; Depleted p-channel field effect transistor) that combine sensor and amplifier function in each pixel. This design offers faster readout and lower noise (no charge transfer), allows large collecting areas and flexible data modes.

Microcalorimeters I

Microcalorimeter: Directly measure heat deposited by single X-ray photon.

Temperature jump depends on the X-ray photon energy (1 keV = 1.6×10^{-9} erg) and heat capacity ($c_V = 3Nk$; 1 mm^3 of Si: N = 5×10^{19}):

$$\Delta T = \frac{E}{c_V} = \frac{1.6 \times 10^{-9}\,\mathrm{erg}}{2 \times 10^{4}\,\mathrm{erg/K}} \approx 8\times10^{-14}\,\mathrm{K}!? \tag{4}$$

What's wrong?

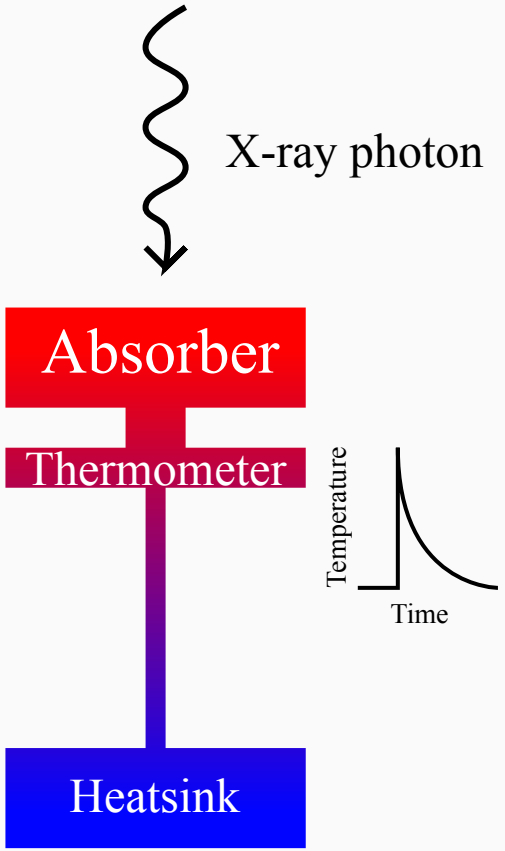

Microcalorimeters II

$\rightarrow$ Cool absorber close to absolute zero: introduces quantum mechanical effects (vibrational states of atoms are quantized), decreases heat capacity.

$$c_V \sim 234\, Nk\left(\frac{T}{\theta_D}\right)^3 \tag{5}$$

Therefore, at a temperature of 0.1 K (the Debye temperature, $\theta_D = 640$ K for silicon), $c_V \sim 6 \times 10^{-6}$ erg/K. Thus,

$$\Delta T = \frac{E}{c_V} = \frac{1.6 \times 10^{-9}\,\mathrm{erg}}{6 \times 10^{-6}\,\mathrm{erg/K}} \approx 3 \times 10^{-4}\,\mathrm{K}, \tag{6}$$

which is measurable. Hurray for QM!

Microcalorimeters III

The biggest advantage of using microcalorimeters is the energy resolution.

Remember from above that (because of counting statistics): $\Delta E/E \sim \Delta N/N = 1/\sqrt{N}$.

In cooled microcalorimeters the heat is converted to the quantized movements of the atoms, i.e. *phonons*, and the number of phonons is proportional to the kinetic energy of the incoming X-ray photon (assuming 100% absorption efficiency). The single phonon has an energy of $E_{phonon} = kT$, where T is the temperature of the absorber. Thus, the number of phonons produced is $N = E/kT$. From above: $\Delta T = E/c_V$, and $c_V \sim T^3$:

$$\frac{\Delta E}{E} \sim \frac{1}{\sqrt{N}} \rightarrow \Delta E \sim \frac{E}{\sqrt{E/kT}} = \sqrt{\Delta T c_V kT} \sim \sqrt{T^5} \qquad (7)$$

The energy resolution depends mostly on the detector temperature.

Microcalorimeters IV

Other requirements for the detector:

- The absorbing material must thermalize quickly and reproducibly. The detector needs to cool down fast in order to detect the next photon.
- Compromise between size and heat capacity: better collection efficiency when larger volume, but leads to larger heat capacity and lower energy resolution.
- Active control of the temperature of the detector (accuracy of $\sim \mu$K). Must be much smaller than ΔT.
- Non-imaging, thus requires many detectors to provide some spatial resolution.

Microcalorimeters V

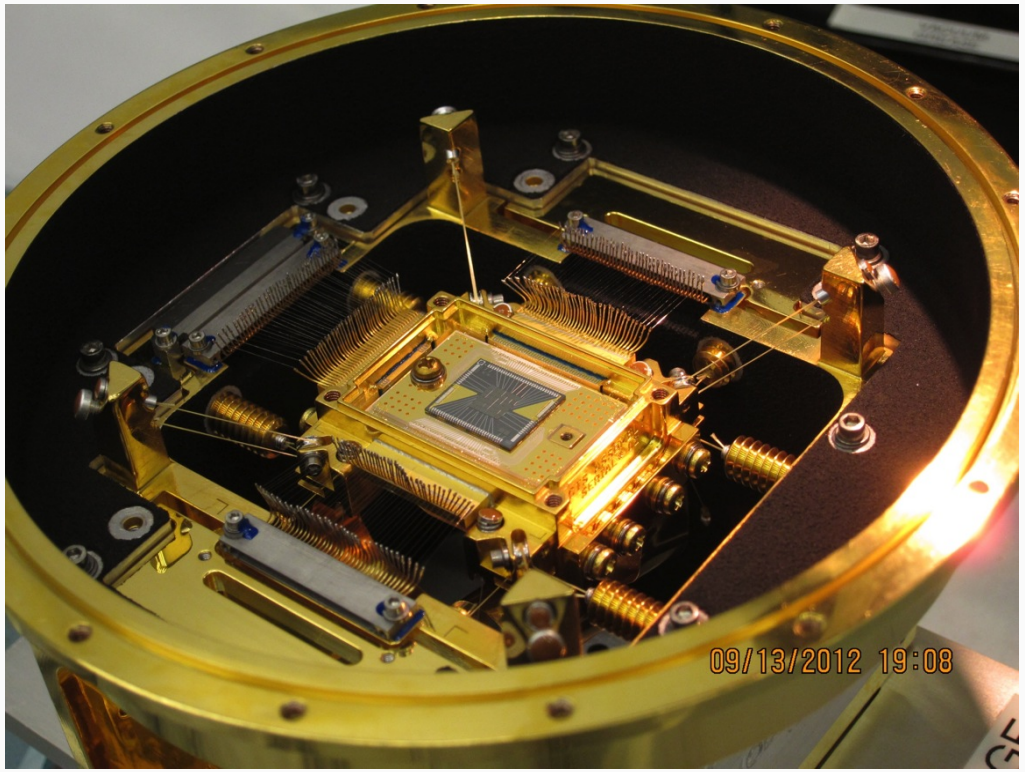

Hitomi XCS (6 $\times$ 6 microcalorimeter array) inside dewar. Operating temperature 50 mK.

Microcalorimeters VI

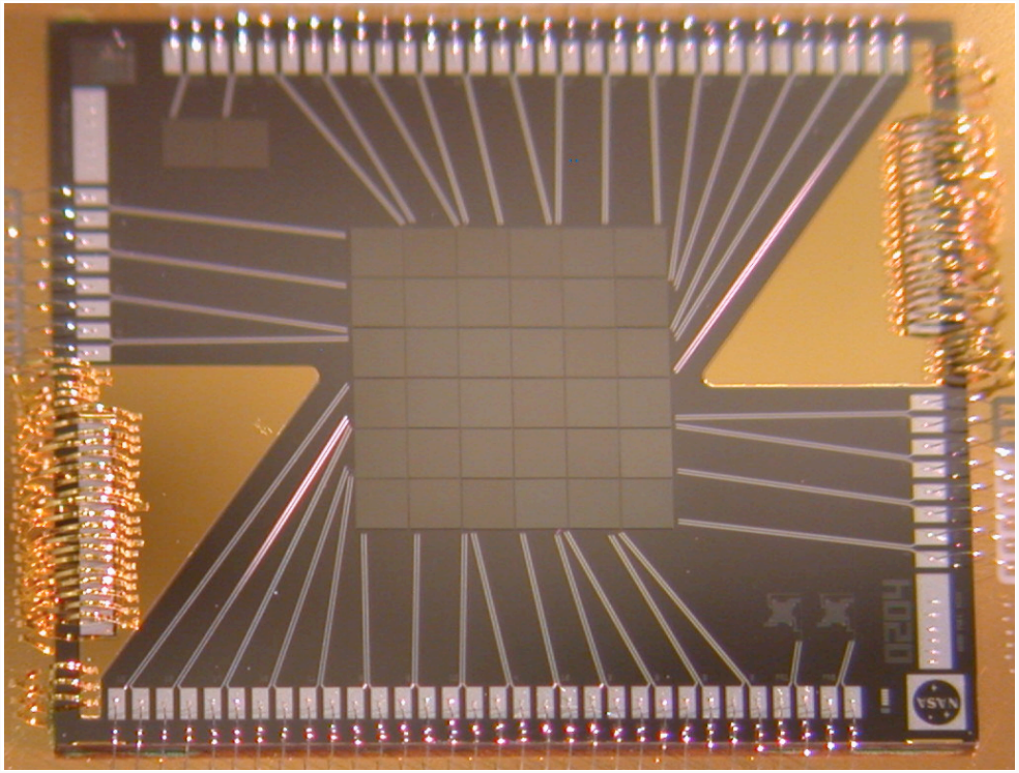

The microcalorimeter array zoom-up showing the absorbers and heat sinking. Absorbers: semi-metal HgTe. Pixel size: 814 $\times$ 814 μm. Thickness 8 μm. $c_V = 6 \times 10^{-7}$ erg/K. $\Delta E = 4.2$ eV. Pulse fall time = 3.5 ms.

Microcalorimeters VII

Thermistors under the absorbers. Four silicon support beams to the heatsink.

Microcalorimeters: Conclusion

Pros: The highest energy resolution available.

Cons: Lower timing accuracy compared to proportional counters, 90% efficiency, non-imaging.

Spectral range: 0.1–10 keV.

Examples: Suzaku XRS (didn't work because of coolant leak), Hitomi XCS (observed one source before the control of the satellite was lost)

Microcalorimeters: Future

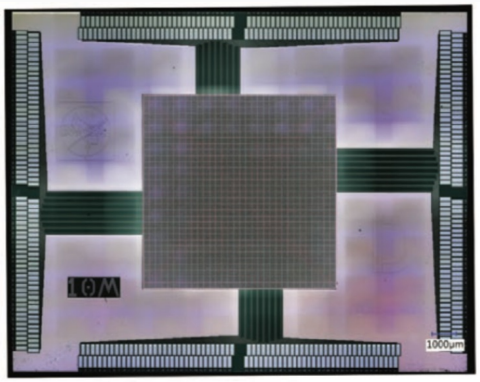

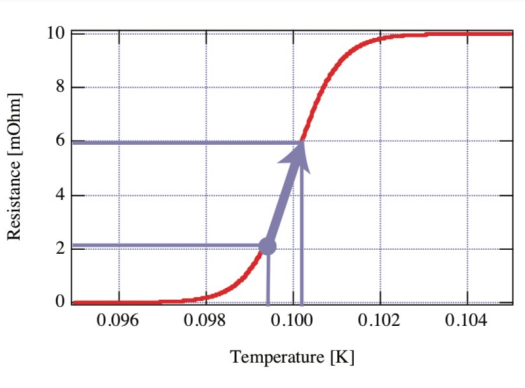

The other focal plane instruments onboard *Athena* will be the X-ray Integral Field Unit (X-IFU). XIFU will host an array of $\sim$3000 microcalorimeters using a Transition-Edge Sensor (TES) technology. In TES, a thin metal film is operated at its superconducting transition, so that any tiny increase in temperature will produce a relatively large change in resistivity which is measured. TES-based detectors can achieve $\Delta E < 2.5$ eV at 0.2–7 keV.

Optics

Earth/Moon occultation I

The diameter of Earth occults roughly 30 % of the sky at any one time from low-Earth orbit. Uncollimated detector measures the visible sky brightness. As spacecraft moves around Earth, X-ray sources 'rise' and 'set' behind Earth changing the sky brightness.

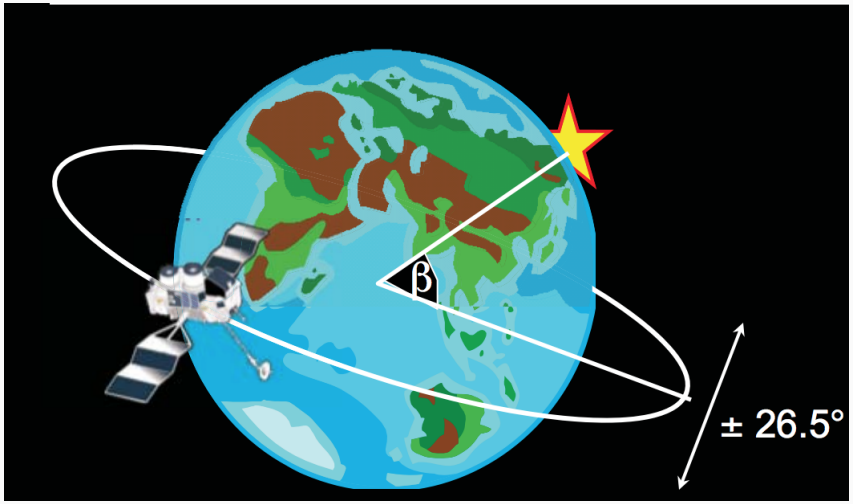

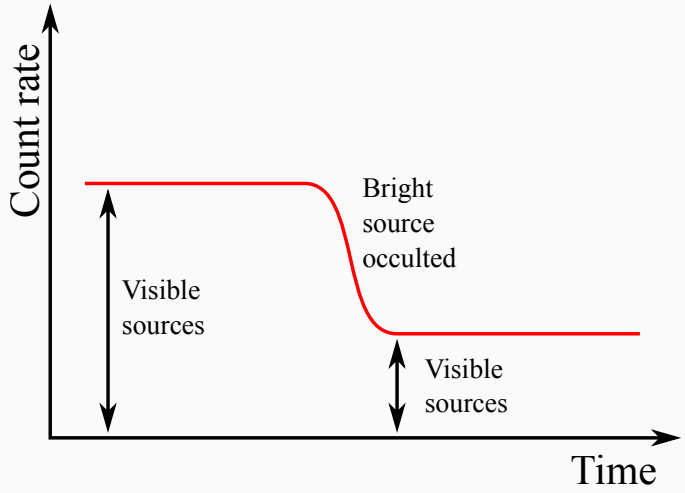

The precession of the orbit shifts the portion of the occulted sky, so that the whole sky is occulted in $\sim$ 50 days.

Earth/Moon occultation II

- Lunar occultations used in 60s and 70s to measure the extent and structure of the supernova remnant Crab nebula and a few, bright X-ray binaries.
- Earth occultation still used today, e.g. in Fermi GBM.
- Bright sources are easy, fainter sources needs background modeling and maximum likelihood methods for possible detections and comparison to catalogues.

Collimators I

- Proportional counters are undirectional to X-ray photons, so collimators/windows are used.
- At energies above $\sim$ 10 keV, imaging with mirror systems not technically possible.
- Simplest method: honeycomb collimator (pin-hole camera).
- Field-of-view: FOV $\sim d/h$. Usually degrees.

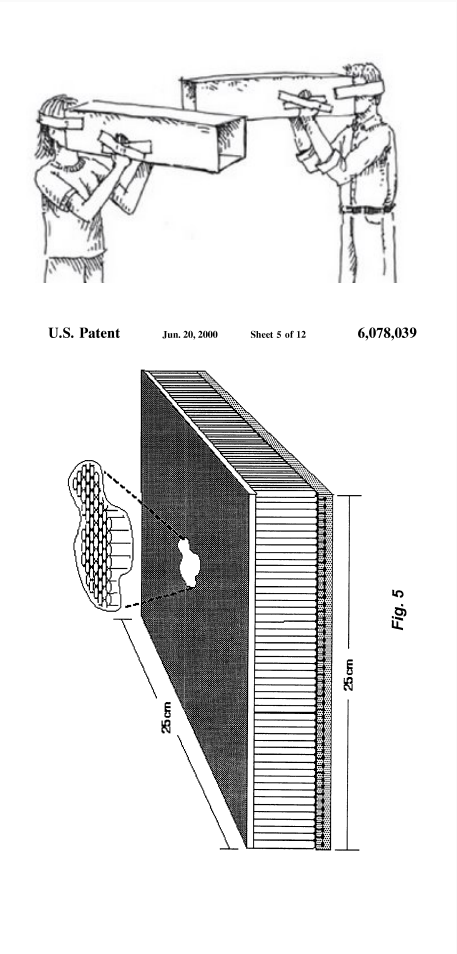

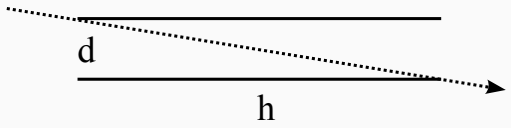

Imaging: Collimators II

- Problem of collimators: no imaging capabilities.
- One solution is to use coded masks: combination of holey mask (hallelujah!) and position sensitive detector.
- Computational image reconstruction. Masks are optimized to allow source reconstruction with high signal-to-noise ratio (as holey as possible).

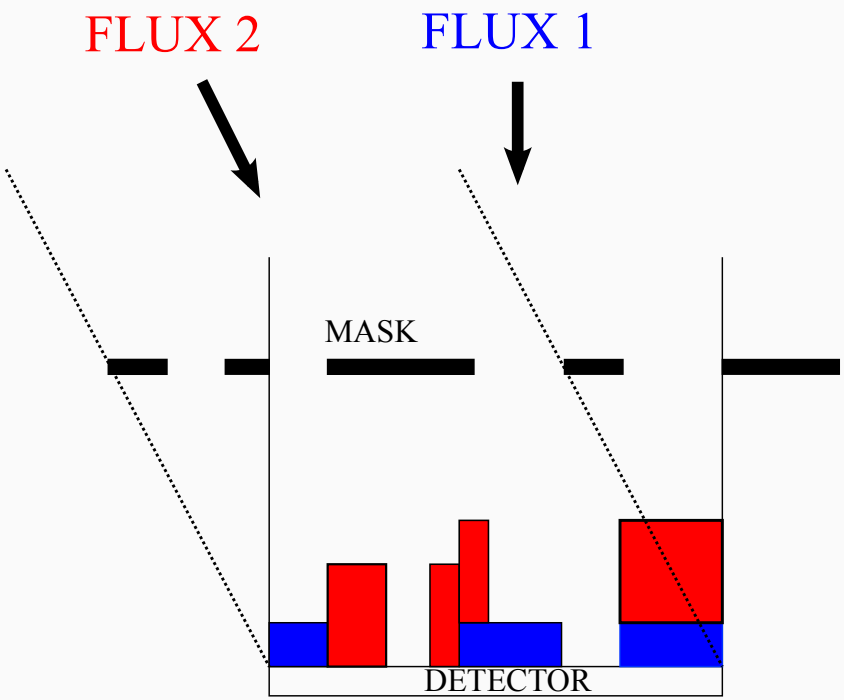

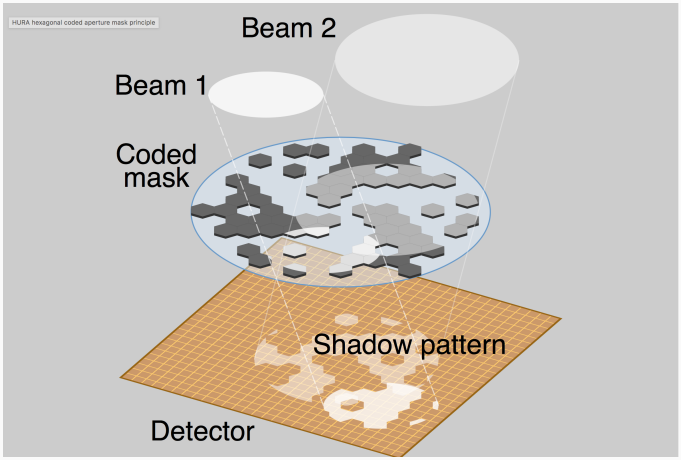

Collimators III

Swift/BAT coded mask.

Wolter telescopes I

Optical telescopes are reflectors. Reflection occurs when the incoming wavefront angle to the surface is less than a critical angle for total reflection.

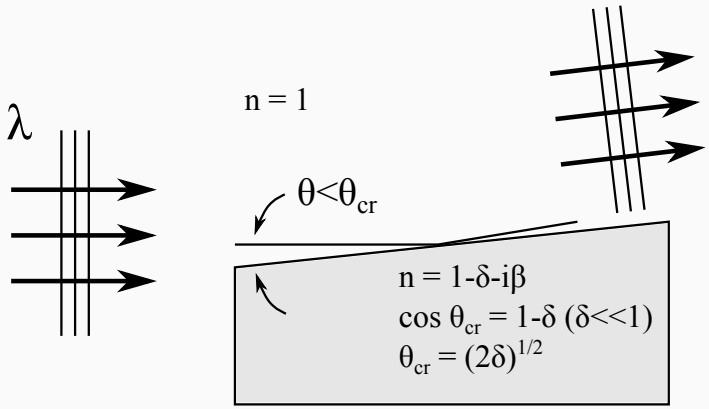

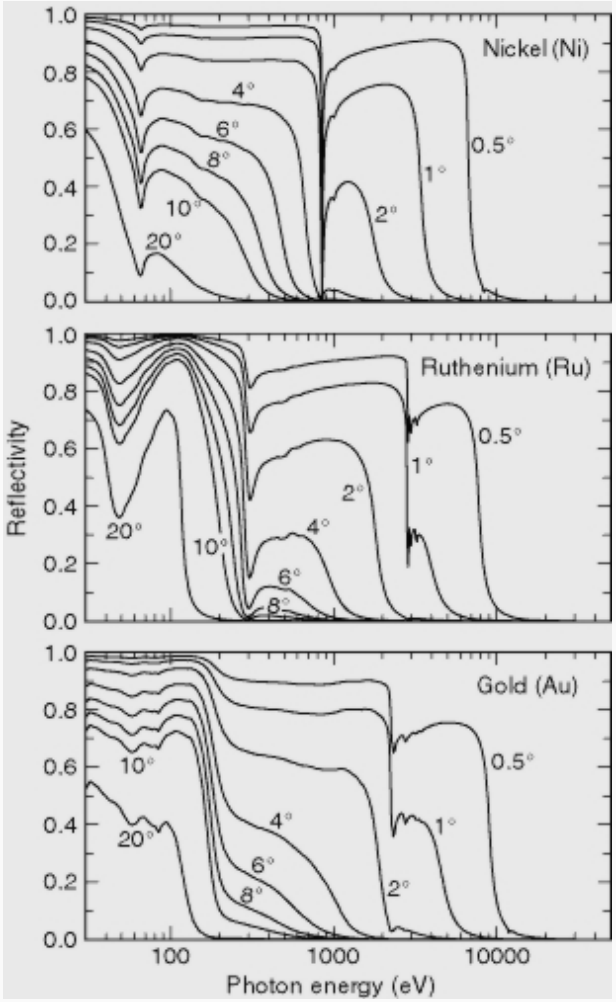

For X-rays, this angle is very small. The critical angle is dependent on the reflecting material and the photon wavelength. The angle becomes 0° for X-rays $\geq$10 keV.

$$\theta_{cr}[arcmin] \approx 5.6\lambda[\AA]\sqrt{\rho[g/cm^3]} \qquad (8)$$

Wolter telescopes II

Small angle reflection $\rightarrow$ grazing incidence X-ray telescopes (cf. skipping stones).

To obtain reasonable focal lengths ($\sim$10 m) requires two reflections in a so-called Wolter type I configuration.

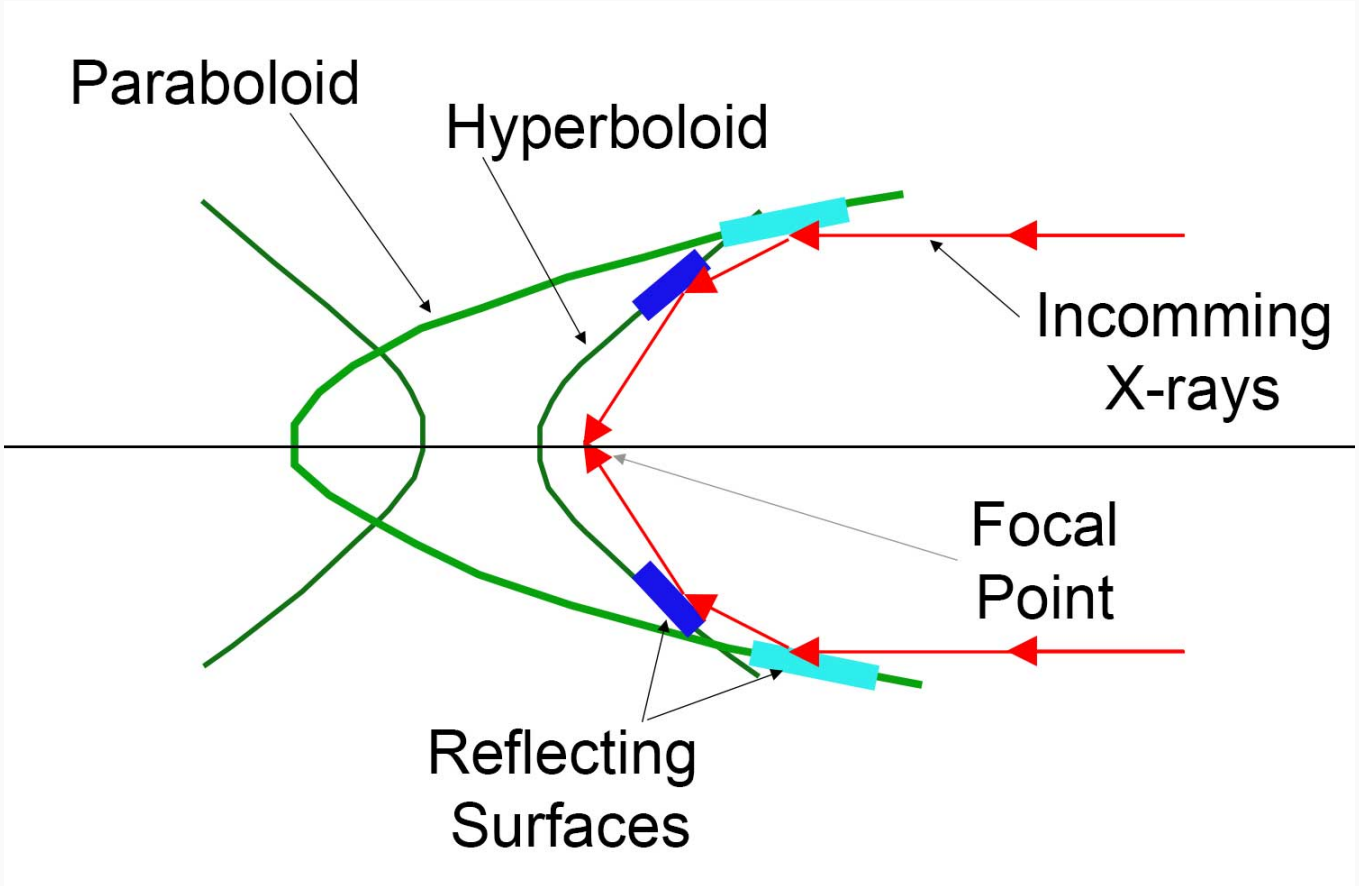

Wolter telescopes III

Problem: Because of the requirement of grazing incidence most of the X-ray photons strike the telescope in wrong angles.

Solution: Nested mirror assembly.

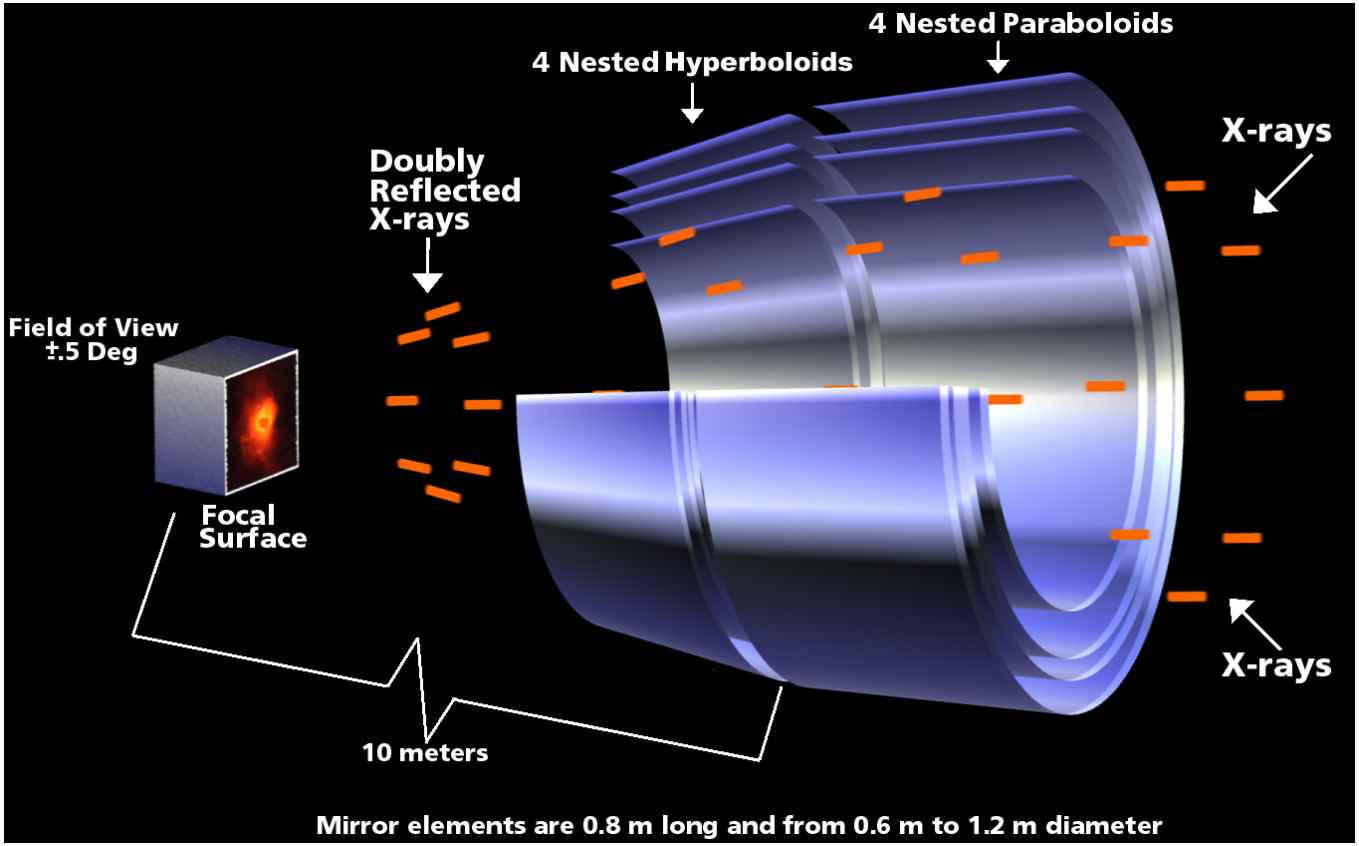

(Illustration: NASA/CXC/D.Berry)

Wolter telescopes IV

Ramping up: Chandra (4 nested mirrors), XMM-Newton (58 mirrors), NuSTAR (133 mirrors), Suzaku (175 mirrors).

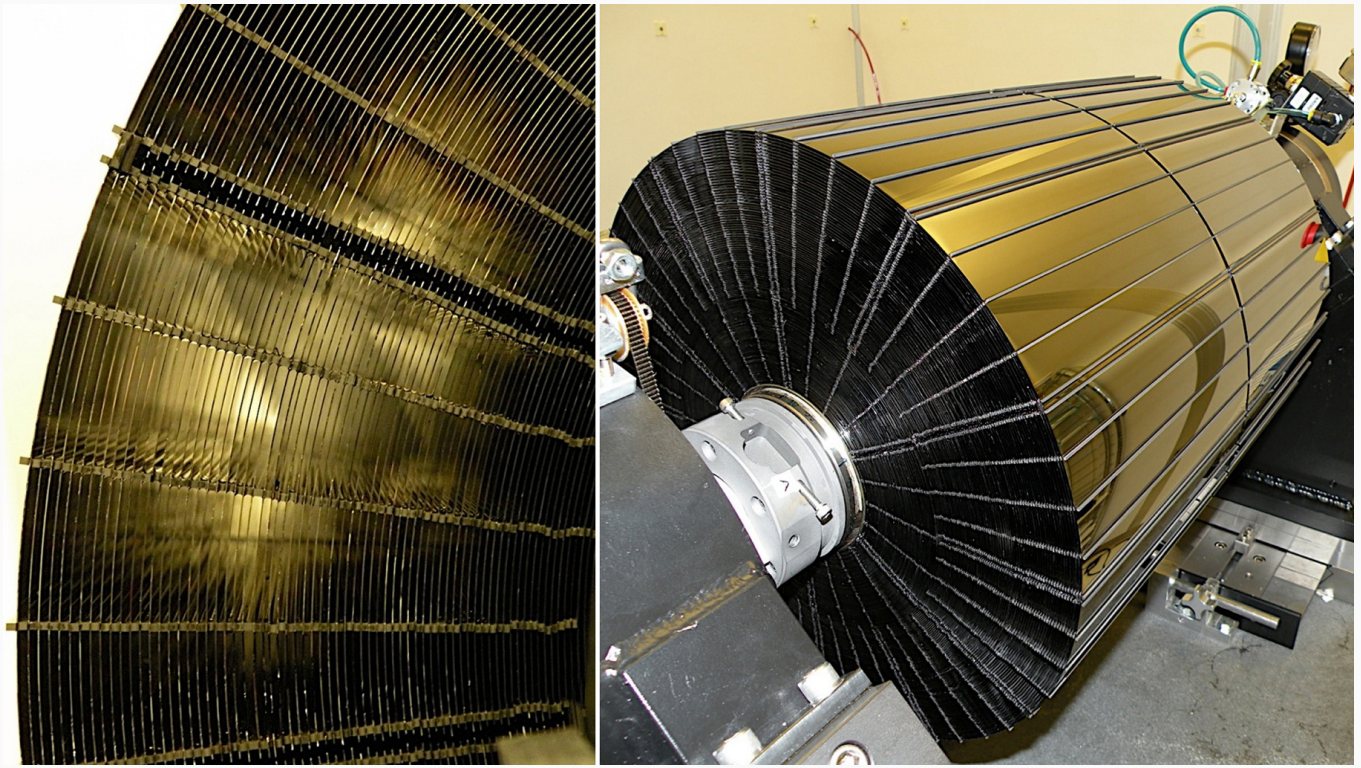

(Image credit: NASA/JPL-Caltech)

Wolter telescopes V

Chandra/XMM-Newton/Suzaku used iridium/gold for high reflectivity, but for low X-ray energy photons.

NuSTAR uses depth-graded multilayer mirror coatings, i.e. thin coatings ($\sim$200) of two alternating materials with high (W, Pt) and low (Si, C) densities deposited one on top of the other.

Multilayer stack acts as a crystal lattice and constructive interference creates enhanced reflectivity.

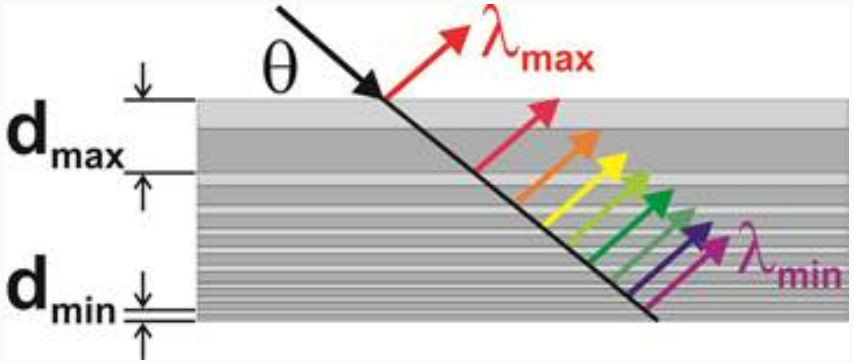

Wolter telescopes: Future

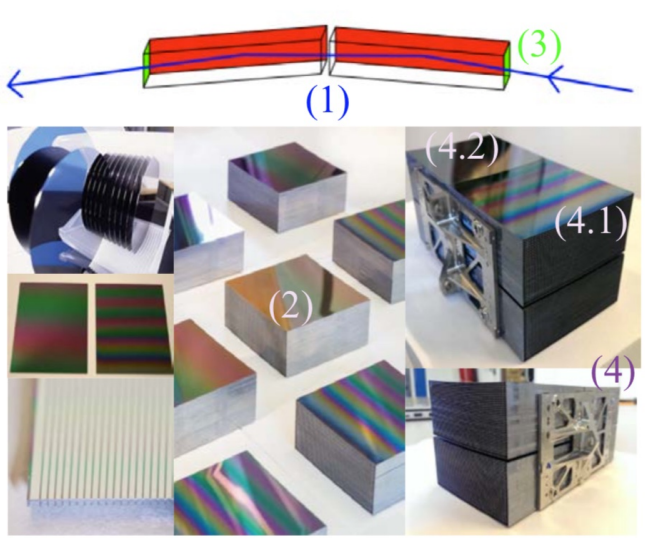

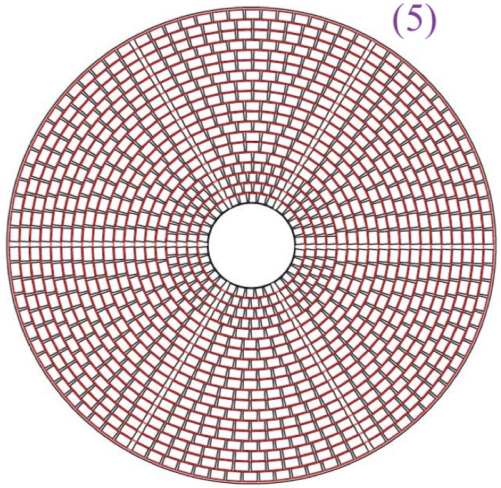

Athena will have the largest X-ray mirror ever built, with an aperture diameter of 3 m, which is made of Silicon Pore Optics (SPO). The SPO mirror is made of commercially available silicon wafers that are diced and grooved to procude Si mirror plates. The wafers are stacked with an aperture split into pores. Two stacks are aligned to form Wolter configuration. The *Athena* mirror will consist of more than a thousand of these stacks with a total of $\sim$2.6 million pores (reflecting surface $\sim$ two tennis courts).

Diffraction gratings I

Conventional dispersed spectroscopy possible using transmission or reflection gratings (at grazing incidence).

Gratings are placed in between the mirror and the detector.

The position of the peaks of the diffraction pattern on the detector gives the wavelength (i.e. energy) of the X-ray photon:

$$m\lambda = b(\sin\beta) \approx bx/F \qquad (9)$$

m = diffraction order, b = groove spacing / slit separation, x = distance between peaks, F = focal length.

Increasing the number of slits (N) results in narrower peaks.

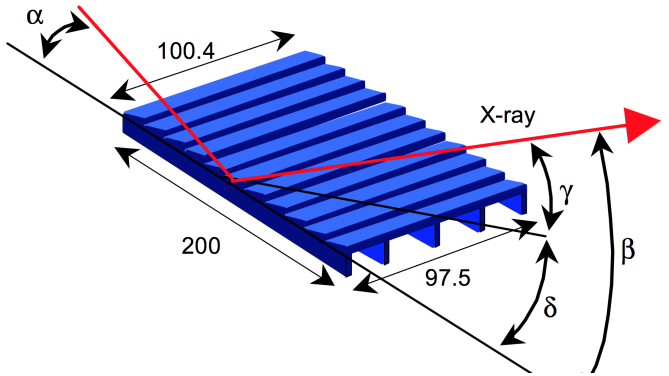

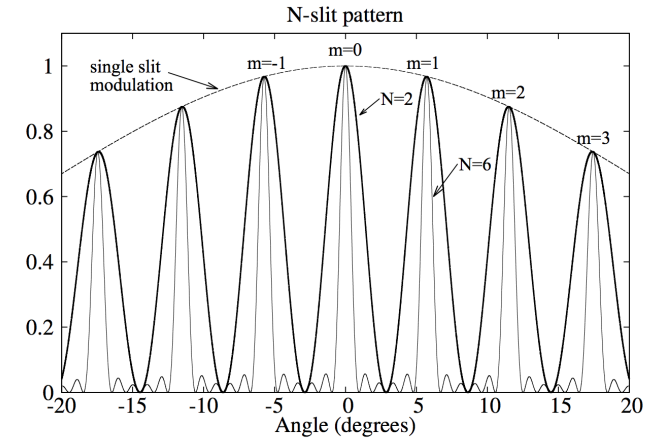

Diffraction gratings II

Spectral resolution: can we resolve the diffraction pattern of two neighboring wavelengths?

Distinguishing two photons from each other (i.e. two diffraction patterns) requires resolving the diffraction peaks. The width of the peak is narrower for larger N, and the displacement is dependent on the wavelength of the photon:

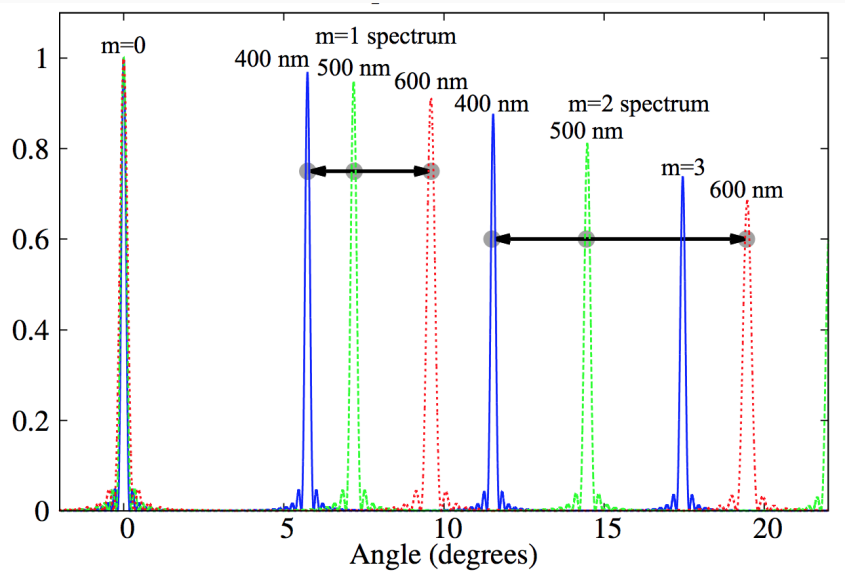

$$\Delta E = \Delta\lambda = \frac{\lambda}{Nm} \qquad (10)$$

Better sensitivity when using higher diffraction orders. However, these are less luminous.

References and further reading

References and further reading

- www.black-hole.eu → Schools, Workshops, and Conferences → 1st & 2nd School on Multiwavelength Astronomy
- Jörn Wilms' lecture pages: http://pulsar.sternwarte.uni-erlangen.de/wilms/teach/index.html (e.g. X-ray Astronomy I, 2008)
- Danny Steeghs' lecture pages: https://www2.warwick.ac.uk/fac/sci/physics/research/astro/people/steeghs/mpags-as2/
- X-ray data booklet, http://xdb.lbl.gov/, Lawrence Berkeley National Laboratory
- Arnaud, K., Smith, R., Siemiginowska, A., 2011, Handbook of X-ray astronomy, Cambridge University Press
- Hard core: Knoll, G. F., 2000, Radiation Detection and Measurement, 4th edition, New York: Wiley